

Femtosecond transmission spectroscopy at the direct band edge of germanium

Gary Mak and Henry M. van Driel

*Department of Physics, University of Toronto and Ontario Laser and Lightwave Research Centre,
Toronto, Ontario, Canada M5S 1A7*

(Received 19 January 1994; revised manuscript received 23 March 1994)

We time-resolve the transient, photoinduced transmission near the direct band edge of crystalline germanium (at 295 K) with 120-fs, tunable, infrared pulses from a 76-MHz optical parametric oscillator. The data show a rich collection of phenomena including band-gap renormalization, carrier-carrier scattering, carrier cooling, and $\Gamma \rightarrow L$ intervalley scattering. An apparent carrier-density dependence in the measured intervalley scattering time is attributed to plasma screening of the Coulomb enhanced continuum absorption.

The ultrafast properties of germanium have attracted renewed interest, both fundamentally and technologically (e.g., Si-Ge alloys for high-speed electronics). Relatively less is known about the ultrafast carrier kinetics in indirect-band-gap materials, than, say, III-V direct-band-gap materials such as GaAs, upon which the majority of ultrafast optical and electronic studies have concentrated. To date, there have been limited optical investigations of germanium with subpicosecond resolution.¹⁻⁵ Part of the problem has been the lack of suitable optical sources. In these experiments, we exploit a femtosecond, infrared, optical parametric oscillator⁶ to measure time-resolved transient photoinduced transmission near the Ge direct band edge. The results reveal a wide range of phenomena: band-gap renormalization, two-photon absorption, carrier-carrier scattering, carrier cooling, and intervalley scattering.

In particular, we observe a manifestation of the intrinsic Coulomb interaction between charged carriers. The optical absorption in semiconductors is profoundly modified by Coulomb effects, with implications for interpreting femtosecond time-resolved spectroscopy experiments.⁷⁻⁹ The Coulomb interaction, which leads to excitonic bound states and an enhancement of the continuum absorption (see, e.g., Ref. 10), can be screened by an electron-hole plasma. We measure a pronounced carrier density dependence ($n \sim 10^{15} - 10^{17} \text{ cm}^{-3}$) in the temporal recovery of the transient photoinduced transmission, which we attribute to plasma screening.^{11,12} Indirect-band-gap Ge is ideal for studying plasma screening as the Coulomb enhancement is strongest near the band edge, and the intervalley scattering acts as an effective "clock" for the Γ -electron density decay.

The time-resolved photoinduced transmission experiments are performed in the usual pump-probe geometry. Tunable (1.2–1.7 μm), 120-fs pulses at 76 MHz from our optical parametric oscillator are split into a pump and a probe beam, which can be parallel- or cross-linear-polarized, and are focused to a 30- μm spot radius. We emphasize that in a given experiment the pump and probe pulses have the same wavelength. The transmitted probe beam and a reference beam are detected by In-Ga-As *p-i-n* detectors and differentially amplified. The probe pulses are time-delayed by rapidly scanning an optical delay line consisting of a speaker driven at 15 Hz.

The speaker driver triggers a computer controlled digital acquisition board which samples and averages $\approx 10^4$ traces. All measurements are done at room temperature. Two polished intrinsic germanium samples are used: one 21 μm thick, the other, 3.5 μm thick. For optical excitation at energies larger than the direct band edge (0.80 eV), electrons are generated in the Γ valley and holes in the valence band. (This contrasts with the equilibrium electron population in the $4L$ valleys; indirect band gap 0.66 eV.) The maximum surface carrier density in these measurements is estimated to be 10^{17} cm^{-3} . All changes in transmission are attributed to absorption changes $\Delta\alpha$, i.e., $\Delta T/T = \exp(-\Delta\alpha L) - 1 \approx -\Delta\alpha L$, which we have verified with complementary time-resolved reflectivity measurements. The carrier lifetime in these samples is limited by surface recombination to ≈ 100 ps, which is much less than the 13-ns pulse repetition time.

Plotted in Figs. 1(a)–(c) is the time-resolved differential transmission of the thick Ge sample at a maximum fluence of $F_0 = 7 \mu\text{J}/\text{cm}^2$ and at wavelengths below ($\lambda = 1.65 \mu\text{m}$), at ($\lambda = 1.55 \mu\text{m}$), and above ($\lambda = 1.48 \mu\text{m}$) the direct band edge, respectively. Below the direct band edge, we see an instantaneous absorption which follows the pulse intensity autocorrelation function. The side lobes are due to secondary reflections, observed because of the low absorption. The peak $\Delta\alpha$ scales linearly with pump fluence, indicative of two photon absorption. The estimated two photon absorption coefficient is $\approx 100 \text{ cm}/\text{GW}$, which is comparable to that calculated using a universal model fitted to numerous semiconductors.¹³ At the band edge, we see an initial rapid absorption followed by a strong bleaching and recovery. The initial absorption results from instantaneous, carrier-induced band-gap renormalization. It is distinguished from two photon absorption by the larger magnitude and the intensity dependence (Fig. 2) which is sublinear relative to the bleaching due to linear band filling. The large valence-band density of states and long hole lifetime reduces the role of holes in these experiments. Thus, the dominant absorption changes on a femtosecond time scale are attributed to the behavior of Γ electrons. The bleaching due to a density of Γ electrons n recovers in a few hundred femtoseconds as they scatter to the L valley via zone boundary phonon emission. The $\Gamma \rightarrow L$ electron intervalley scattering time $\tau_{\Gamma V}$ is defined

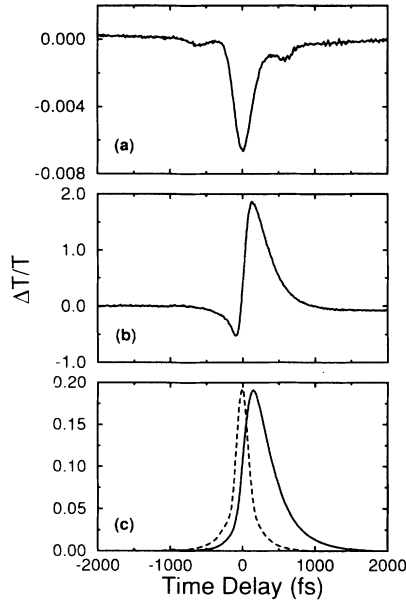


FIG. 1. Time-resolved differential transmission at maximum fluence (F_0) and three different wavelengths: below the direct band edge [$\lambda=1.65 \mu\text{m}$; (a)], at the band edge [$\lambda=1.55 \mu\text{m}$; (b)], and above the band edge [$\lambda=1.48 \mu\text{m}$; (c)]. The dashed curve in (c) is the pulse intensity autocorrelation function at that wavelength.

by $n(t) = n_0 \exp(-t/\tau_{IV})$. Above the band edge, only the bleaching signal is present. Figures 2(a) and (b) illustrate band-edge traces for $F_0/3$ and $F_0/10$. They clearly show the sublinear behavior expected of band-gap renormalization as well as carrier cooling. After the Γ electrons scatter into the L valley, they become hot (≈ 1100 K) and cool to the lattice temperature on a picosecond time scale.¹ These cooling carriers contribute to picosecond band-gap renormalization and absorption for $t > 1$ ps. Also plotted in Fig. 1(c) is the pulse intensity autocorrelation function at that wavelength. The width (185 fs) represents an upper limit over which the coherent artifact may contribute to the data. Clearly it does not strongly influence the bleaching decay or the picosecond band-gap renormalization. Further, the coherent artifact scales linearly with fluence, whereas the band-gap renormalization signal does not.

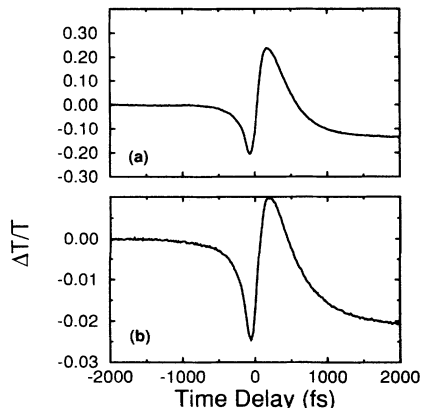


FIG. 2. Differential transmission at the band edge ($\lambda=1.55 \mu\text{m}$) at reduced fluence $F_0/3$ (a) and $F_0/10$ (b).

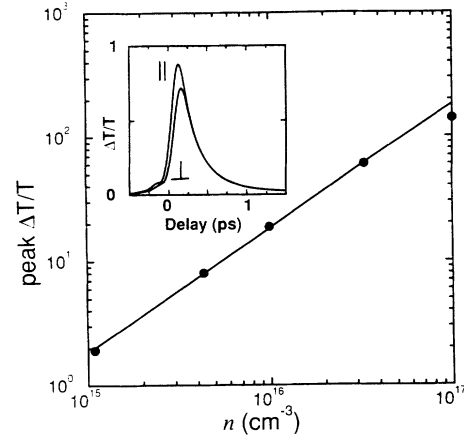


FIG. 3. Peak bleaching vs carrier density at $\Delta E = 35$ meV. Solid line has a slope of 1. Inset shows the transmission for pump and probe beams parallel and cross-polarized ($n \approx 10^{17} \text{cm}^{-3}$).

One might expect that τ_{IV} can be extracted directly from an exponential fit to the bleaching decay, assuming band filling dominates ($\Delta\alpha \propto n$). To test this hypothesis, we measure the differential transmission vs fluence from F_0 to $F_0/100$. We probe above the band edge ($\lambda=1.48 \mu\text{m}$; excess energy above the band edge $\Delta E=35$ meV), in order to minimize band-gap renormalization and carrier cooling effects, and use the thin Ge sample to compensate for the increased absorption. As plotted in Fig. 3, the peak bleaching signal depends almost linearly on carrier density, except at maximum excitation where carrier-carrier scattering becomes efficient¹⁴ (see below). The surprising feature is that the *measured* intervalley scattering time τ_m increases with decreasing excitation [Fig. 4 (curve A)].

We stress that τ_{IV} should be independent of n except at very high densities ($> 10^{19} \text{cm}^{-3}$). Carrier population (final state band filling) and nonequilibrium phonon effects which could increase τ_{IV} are expected to be small here, because of the large L -valley density of states. Also, both mechanisms would produce the opposite effect; increasing τ_m with increasing excitation. The deformation

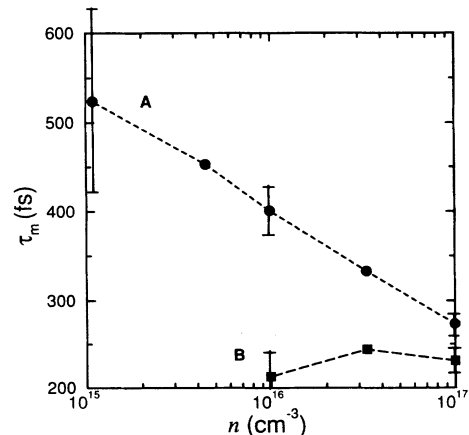


FIG. 4. Measured exponential decay times of the photoinduced bleaching vs carrier density at two energies above the band edge; $\Delta E = 35$ meV (curve A) and $\Delta E = 7$ meV (curve B).

potential phonon scattering is unscreened to first order.

Carrier-carrier scattering and thermalization, which remove carriers from the optically excited region, could play a role in the density dependence. Evidence for carrier-carrier scattering is seen at the maximum fluence where the peak bleaching becomes slightly sublinear with carrier density (Fig. 3) and the difference between the parallel and cross-polarized transmission traces show no absorption anisotropy¹⁵ after the peak bleaching (inset to Fig. 3), i.e., there is rapid momentum space redistribution (although not necessarily, energy redistribution). However, it is clear that carrier-carrier scattering is less important at lower density. An additional check that the density variation of τ_m is not due to carrier-carrier scattering is to measure at the band edge where there is reduced phase space for carrier-carrier scattering. The band-edge transmission for $n \simeq 10^{17} \text{ cm}^{-3}$ (Fig. 5) shows pronounced absorption anisotropy during the decay of the transmission bleaching indicating that carrier-carrier scattering does not dominate the decay. The average, bleaching, exponential decay time of the parallel and cross-polarized traces is 230 fs, although this is probably an upper limit due to convolution with the picosecond band-gap renormalization response.

It is interesting that τ_m at the band edge is shorter than that at higher excitation energy [Fig. 4 (curve A)]. To explore this further, we probe slightly above the band edge ($\Delta E = 7 \text{ meV}$) in order to minimize the band-gap renormalization signal as much as possible and determine τ_m vs carrier density [Fig. 4 (curve B)]. We obtain a density independent (within experimental uncertainty) decay time of about $\simeq 230 \text{ fs}$, over one order of magnitude carrier density variation.

We can explain these results by considering that the linear band filling does not necessarily dominate the bleaching of the transmission. For the results at $\Delta E = 35 \text{ meV}$, if the change in absorption depends on the carrier density as

$$\Delta\alpha \propto n^\gamma = n_0^\gamma \exp(-t/\tau_m) \quad (1)$$

then $\tau_m = \tau_{IV}/\gamma$ and in general $\gamma = \gamma(n)$. This is the case when plasma screening is taken into account.

The bleaching signal has a contribution from plasma screening of the Coulomb enhancement of the contin-

uum absorption.^{11,12} The above band-edge absorption has been derived in a non-many-body, plasma theory and is given by¹⁰

$$\alpha(\omega) \propto \frac{\sinh(\pi g \sqrt{x})}{\cosh(\pi g \sqrt{x}) - \cos(\pi \sqrt{4g - xg^2})} [1 - f_e - f_h]. \quad (2)$$

Here $x = (\hbar\omega - E'_g)/E_0$, E_0 is the exciton Rydberg with Bohr radius a_0 , f_α is the electron ($\alpha=e$) and hole (h) Fermi occupation factor, E'_g is the renormalized direct band gap, $g = \Omega/a_0q_D$ is a screening strength parameter, and q_D is the screening wave vector, which in the static, classical limit is the Debye-Hückel wave vector $q_D = (e^2n/\epsilon k_B T)^{1/2}$. The last bracketed term in Eq. (2) is the band-filling term, such that $\Delta\alpha \propto -f_e$, which is linear with n in the nondegenerate regime. The leading factor in Eq. (2) is the Coulomb modified continuum absorption, which yields the expected parabolic band edge ($g \rightarrow 0$) and Wannier ($g \rightarrow \infty$) limits. One can show from this term that $\Delta\alpha \propto -1/\sqrt{g} \propto -\sqrt{n}$; this is the nonlinear plasma screening contribution. Intuitively, in the statically screened picture, the Coulomb potential is scaled by $\exp(-q_D r)$, and thus the Coulomb interaction is reduced by a factor proportional to $q_D \propto \sqrt{n}$.

The total change in absorption can be written as

$$\Delta\alpha \simeq -an - bn^{0.5}, \quad (3)$$

where a and b are positive (and not constants) giving the relative contributions of band filling and plasma screening. Thus according to Eqs. (1) and (3), the measured value of τ_{IV} can be scaled $1 \leq 1/\gamma \leq 2$. Note also, that the linear peak bleaching dependence on carrier density (Fig. 3) is not inconsistent with plasma screening in the static picture; screening is strongest when carriers have been scattered to the band edge after some (internal) thermalization.

We have solved Eq. (2) for γ and compared the calculations with our experiments. Thermalized carrier distributions were assumed. The time-dependent screening (on a femtosecond time scale) is attributed only to the Γ -valley electrons; their low initial carrier temperature is most ef-

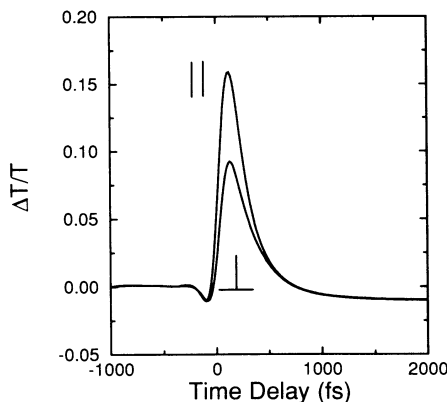


FIG. 5. Parallel and cross-polarized transmission at the band edge ($n \simeq 10^{17} \text{ cm}^{-3}$).

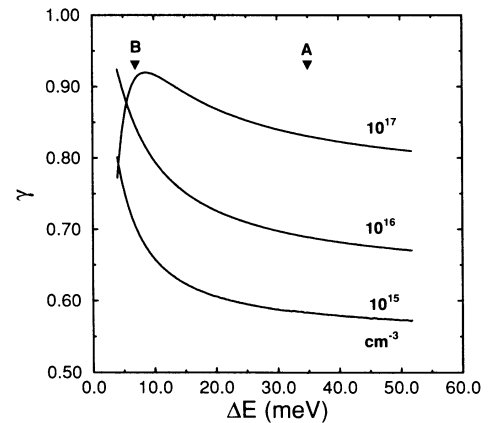


FIG. 6. The calculated power dependence of the absorption bleaching on carrier density γ vs energy above the band edge and as a function of carrier density. The energies which correspond to the experiment are labeled (A, B) as in Fig. 4.

fective at screening in the static limit, which is equivalent to the quasidynamic screening approximation.¹⁶ We have not included band-gap renormalization for excitation above the band edge, since we do not see evidence for enhanced absorption at long times ($t \gg 5$ ps). Plotted in Fig. 6 is the calculated γ vs excitation-probe energy above the band edge and vs carrier density. The calculations show good agreement with the experimental data, and clearly explain the density dependence of the measured time constants at $\Delta E=35$ meV (arrow A), and the much weaker dependence at $\Delta E = 7$ meV (arrow B). We conclude that the $\Gamma \rightarrow L$ electron intervalley scattering time is 230 ± 25 fs, which is consistent with recent femtosecond luminescence upconversion⁵ and four-wave mixing experiments.³ These three measurements contrast

with a Raman scattering measurement of 1.2 ps.⁴

In conclusion, we have measured time-resolved differential transmission following photoexcitation with femtosecond pulses, at the direct band edge of germanium. Coulomb effects, namely, plasma screening of the Coulomb enhanced absorption, affect the accurate measurement of carrier time constants. This has important implications for all ultrafast measurements, absorption, and luminescence near the band edge.

We gratefully acknowledge financial support from the Ontario Technology Fund, NSERC, and Bell-Northern Research Ltd. One of the samples was kindly supplied by A. Smirl.

¹ H. Roskos, B. Rieck, A. Seilmeier, and W. Kaiser, *Appl. Phys. Lett.* **53**, 2406 (1988).

² T. Pfeifer, W. Kütt, H. Kurz, and R. Scholz, *Phys. Rev. Lett.* **69**, 3248 (1992).

³ T. Rappen, U. Peter, M. Wegner, and W. Schaefer, *Phys. Rev. B* **48**, 4879 (1993).

⁴ K. Tanaka, H. Ohtake, and T. Suemoto, *Phys. Rev. Lett.* **71**, 1935 (1993).

⁵ X. Q. Zhou, H. M. van Driel, and G. Mak (private communication).

⁶ Q. Fu, G. Mak, and H. M. van Driel, *Opt. Lett.* **17**, 1006 (1992).

⁷ T. Gong, W. L. Nighan, and P. M. Fauchet, *Appl. Phys. Lett.* **57**, 2713 (1990).

⁸ J. Nunnenkamp *et al.*, *Phys. Rev. B* **43**, 14047 (1991).

⁹ C. J. Stanton and D. W. Bailey, *Phys. Rev. B* **47**, 1624 (1993).

¹⁰ H. Haug and S. W. Koch, *Quantum Theory of the Optical and Electronic Properties of Semiconductors* (World Scientific, Singapore, 1990).

¹¹ Y. H. Lee *et al.*, *Phys. Rev. Lett.* **57**, 2446 (1986).

¹² L. Banyai and S. W. Koch, *Z. Phys. B* **63**, 283 (1986).

¹³ E. W. Van Stryland, M. A. Woodall, H. Vanherzeele, and M. J. Soileau, *Opt. Lett.* **10**, 490 (1985).

¹⁴ J. F. Young, T. Gong, P. J. Kelly, and P. M. Fauchet (private communication).

¹⁵ J. L. Oudar *et al.*, *Phys. Rev. Lett.* **53**, 384 (1984); A. J. Taylor, D. J. Erskine, and C. L. Tang, *J. Opt. Soc. Am. B* **2**, 663 (1985).

¹⁶ M. Ulman *et al.*, *Phys. Rev. B* **47**, 10267 (1993).